

# A linear barycentric rational interpolant on starlike domains

Jean-Paul Berrut\*      Giacomo Elefante\*

## Abstract

When an approximant is accurate on the interval, it is only natural to try to extend it to several-dimensional domains. In the present article, we make use of the fact that linear rational barycentric interpolants converge rapidly toward analytic and several times differentiable functions to interpolate on two-dimensional starlike domains parametrized in polar coordinates. In radial direction, we engage interpolants at *conformally shifted Chebyshev nodes*, which converge exponentially toward analytic functions. In circular direction, we deploy linear rational trigonometric barycentric interpolants, which converge similarly rapidly for periodic functions, but now for *conformally shifted equispaced nodes*. We introduce a variant of a tensor-product interpolant of the above two schemes and prove that it converges exponentially for two-dimensional analytic functions—up to a logarithmic factor—and with an order limited only by the order of differentiability for real functions, if the boundary is as smooth. Numerical examples confirm that the shifts permit to reach a much higher accuracy with significantly less nodes, a property which is especially important in several dimensions.

Interpolating a function in several dimensions is a fundamental research topic in applied mathematics, due to its many applications in engineering, data science and many other fields.

In the present work, we shall merely be interested in infinitely smooth interpolants. For the abundant literature on splines, the reader may consult [31], among the many books on the subject.

The problem is very much dependent on the choice of the nodes and a lot of research has been done in this field. In the square  $[-1, 1]^2$ , a well-known points set for Lagrange interpolation is given by the Padua points [13]. These nodes allow the unique interpolation in the space  $\mathbb{P}_n^2$  of polynomials in two variables of degree less than or equal to  $n$  and achieve a Lebesgue constant with a slow growth of  $\mathcal{O}(\log^2 n)$ . One of their peculiarities, useful for applications such as MPI [15], is that they can be defined as well as the intersection of the Lissajous curve

$$\gamma(t) = \left( \cos(nt), \cos((n+1)t) \right), \quad t \in [0, \pi],$$

with itself and the boundary of the square  $[-1, 1]^2$ . Bos et al. [11] have studied the generalisation to the  $d$ -dimensional cube.

---

\*Department of Mathematics, University of Fribourg, Fribourg, Switzerland (jean-paul.berrut@unifr.ch, giacomo.elefante@unifr.ch).

Recently, Erb et al. [19, 21] have studied a generalisation of the theory of Padua points to classes of points generated by Lissajous curves. We refer the interested reader to [22, 20] and the references therein.

Multivariate rational interpolation has been widely studied as well [14, 1]. As in the unidimensional case, it has the ability to better deal with singularities of the function than polynomials [18]. Unfortunately, rational approximation can be numerically fragile to compute and is inclined to spurious singularities. Many different approaches have been introduced to avoid these drawbacks, such as algorithms based on the singular value decomposition [32] or on a Stieltjes procedure and an optimization formulation [2].

Our idea in the next sections is rather to use the tensor product of linear barycentric rational interpolants, of which it has been proved that they do not have any poles in the real domain of the function.

## 1 Preliminaries

Let us consider  $n+1$  distinct nodes in  $[a, b]$ , which we denote by  $x_i$ ,  $i = 0, \dots, n$ , with their corresponding data  $f_i$ . In case we interpolate a function  $f$  we define the  $f_i$  as  $f_i := f(x_i)$ .

Then, it is well known (see, e.g., [24, p. 238]) that the unique polynomial of degree at most  $n$  interpolating the  $f_i$  may be written in the barycentric form

$$p_n(x) = \frac{\sum_{i=0}^n \frac{\lambda_i}{x-x_i} f_i}{\sum_{i=0}^n \frac{\lambda_i}{x-x_i}}, \quad (1)$$

with the so-called weights  $\lambda_i$  defined by

$$\lambda_i = \prod_{\substack{j=0 \\ j \neq i}}^n \frac{1}{x_i - x_j}.$$

In case the nodes are the Chebyshev points of the second kind, i.e.,

$$x_i = -\cos\left(\frac{i\pi}{n}\right), \quad i = 0, \dots, n,$$

the weights are (up to a constant) [24, p. 252]

$$\lambda_i = (-1)^i \delta_i, \quad (2)$$

with  $\delta_i$  equal to  $1/2$  for the first and the last nodes and to  $1$  for the others.

The interpolant therefore becomes

$$p_n(x) = \frac{\sum_{i=0}^n \prime\prime \frac{(-1)^i}{x-x_i} f_i}{\sum_{i=0}^n \prime\prime \frac{(-1)^i}{x-x_i}}, \quad (3)$$

where the double prime means that the first and the last terms of the sum are halved.

With these nodes,  $p_n$  enjoys excellent convergence properties when the interpolated function is smooth (see, e.g., [33, p. 53]).

**Theorem 1.** *Let  $\nu \geq 1$  be an integer and let  $f$  and its derivatives up to  $f^{(\nu-1)}$  be absolutely continuous on  $[-1, 1]$  and the  $\nu^{\text{th}}$ -derivative be of bounded variation, with  $V$  its total variation. Then for any  $n \geq \nu$  the Chebyshev interpolant satisfies*

$$\|f - p_n\| \leq \frac{4V}{\pi\nu(n - \nu)^\nu}.$$

In the case of functions analytic not only in the interval  $[-1, 1]$  but also in an ellipse with foci  $-1$  and  $1$ , called the *Bernstein ellipse* and denoted by  $E_\sigma$ , where  $\sigma$  is the sum of the lengths of the semiminor and the semimajor axes, the convergence is faster than geometric (see e.g. [29, p. 143]).

**Theorem 2.** *Let  $f$  be a function analytic inside and on an ellipse  $E_\sigma$ . Then for each  $n \geq 0$  the polynomial interpolant between Chebyshev points of the first or the second kind satisfies*

$$\|f - p_n\| \leq \frac{4M}{\sigma^n(\sigma - 1)},$$

where  $M = \max_{z \in E_\sigma} |f(z)|$ .

For other nodes than Chebyshev points, the expression (3) becomes a linear rational interpolant [7]. Baltensperger et al. proved in [4] that the exponential convergence then still holds for Chebyshev nodes shifted with a conformal map, say  $g$ . In fact, in this case we have the following theorem for the interpolant

$$r_n(x) = \frac{\sum_{i=0}^n \frac{(-1)^i}{g(x) - g(x_i)} f(g(x_i))}{\sum_{i=0}^n \frac{(-1)^i}{g(x) - g(x_i)}}. \quad (4)$$

**Theorem 3.** *Let  $\mathcal{D}_1, \mathcal{D}_2$  be two domains of  $\mathbb{C}$  containing  $J = [-1, 1]$ , respectively  $I \subset \mathbb{R}$ , let  $g$  be a conformal map  $\mathcal{D}_1 \rightarrow \mathcal{D}_2$  such that  $g(J) = I$ , and  $f$  be a function  $\mathcal{D}_2 \rightarrow \mathbb{C}$  such that the composition  $f \circ g : \mathcal{D}_1 \rightarrow \mathbb{C}$  is analytic inside and on an ellipse  $E_\sigma \subset \mathcal{D}_1$ ,  $\sigma > 1$ , with foci  $-1$  and  $1$  and with the sum of the semiminor and the semimajor axes equal to  $\sigma$ . Let  $r_n$  be the interpolant (4) interpolating  $f$  at the transformed Chebyshev nodes  $y_i = g(x_i)$ ,  $i = 0, \dots, n$ . Then*

$$\|f - r_n\|_{\infty, [-1, 1]} = \mathcal{O}(\sigma^{-n}).$$

Note that, if we write  $y = g(x)$  and  $y_i = g(x_i)$  for  $i = 0, \dots, n$ , then  $r_n$  can be seen as

$$\tilde{r}_n(y) = \frac{\sum_{i=0}^n \frac{(-1)^i}{y - y_i} f(y_i)}{\sum_{i=0}^n \frac{(-1)^i}{y - y_i}},$$

which corresponds to Berrut's second interpolant [25]  $R_1$ , introduced in [7], at the nodes  $y_i$ .

We now turn to periodic interpolants. For the equidistant nodes

$$\theta_i = i \cdot \frac{2\pi}{n}, \quad \text{for } i = 0, \dots, n - 1, \quad (5)$$

in  $[0, 2\pi)$ , there exists a unique balanced trigonometric polynomial that interpolates the data  $f_i$ ,  $i = 0, \dots, n-1$ , at the nodes, and it can be written in the simple barycentric form

$$T_n(\theta) = \frac{\sum_{i=0}^{n-1} (-1)^i \operatorname{cst}\left(\frac{\theta-\theta_i}{2}\right) f_i}{\sum_{i=0}^{n-1} (-1)^i \operatorname{cst}\left(\frac{\theta-\theta_i}{2}\right)}, \quad (6)$$

where the function  $\operatorname{cst}$  is

$$\operatorname{cst}(\theta) := \begin{cases} \operatorname{csc}(\theta), & \text{if } n \text{ is odd,} \\ \operatorname{ctg}(\theta), & \text{if } n \text{ is even.} \end{cases} \quad (7)$$

Let us define  $\Pi$  as the class of periodic complex valued functions on  $\mathbb{R}$  with period  $2\pi$ . Then, it is possible to prove convergence theorems for  $T_n$  which depend on the smoothness of the function  $f$ , as with Chebyshev interpolation (see [24, p. 365] and [34] for the first theorem and [23] for the second).

**Theorem 4.** *Let  $f \in \Pi$  be such that it has simple jump discontinuities in the  $\mu^{\text{th}}$ -derivative which is of bounded variation  $V$ ; then*

$$|f(\theta) - T_n(\theta)| \leq \frac{V}{\pi m^\mu} \left( \frac{1}{m} + \frac{2}{\mu} \right),$$

with  $m := \lfloor n/2 \rfloor$ .

**Theorem 5.** *Let  $f \in \Pi$  be analytic in the strip  $S_a := \{\eta : |\operatorname{Im}(\eta)| \leq a\}$ , where  $a > 0$ , and  $|f(\theta)| \leq M$ . Then*

$$|f(\theta) - T_n(\theta)| \leq 2M \cot\left(\frac{a}{2}\right) e^{-an}.$$

The first author proposed in [7] to use  $T_n$  for other nodes than equidistant points; then (6) becomes a linear rational trigonometric interpolant, which we denote by  $t_n \equiv t_n[f]$ .

In the wake of the barycentric rational interpolant at the Chebyshev nodes, Baltensperger [3] showed in 2002 that, if we consider as nodes some conformally shifted equidistant points, then the interpolant between these shifted nodes retains the convergence behaviour of the one at equidistant nodes. In fact the following holds.

**Theorem 6.** *Let  $g \in \Pi$  be a conformal map such that  $g(I) = I$  with  $I = [0, 2\pi]$  and such that the function*

$$w(\phi, \theta) := \frac{\operatorname{cst}\left(\frac{g(\phi)-g(\theta)}{2}\right)}{\operatorname{cst}\left(\frac{\phi-\theta}{2}\right)}$$

is bounded and analytic in  $S_{a_1} \times S_{a_1}$  for an  $a_1 > 0$ . Let  $f$  be a function such that  $f \circ g \in \Pi$ . Let

$$t_n(\phi) \equiv t_n[f \circ g](\theta) = \frac{\sum_{i=0}^{n-1} (-1)^i \operatorname{cst}\left(\frac{g(\theta)-g(\theta_i)}{2}\right) f(g(\theta_i))}{\sum_{i=0}^{n-1} (-1)^i \operatorname{cst}\left(\frac{g(\theta)-g(\theta_i)}{2}\right)} \quad (8)$$

be the rational function generalizing (6) between the nodes  $\phi_i := g(\theta_i)$ ,  $i = 0, \dots, n-1$ , where the  $\theta_i$ 's are the equidistant nodes (5). Then for every  $\phi \in I$  we have the following.

- If  $f \circ g$  has simple jump discontinuities in the  $\mu^{\text{th}}$ -derivative, then

$$|f(\phi) - t_n(\phi)| = \mathcal{O}(n^{-\mu}).$$

- If  $f \circ g$  is analytic in a strip  $S_{a_2}$  with  $a_2 \geq a_1 > 0$  and  $f(\phi) \leq M_2$ , then

$$|f(\phi) - t_n(\phi)| = \mathcal{O}(\sigma^{-n}) \quad \text{with } \sigma := e^{a_2}.$$

## 2 The tensor product interpolant and its Lebesgue constant

Let the fixed integer  $d \geq 2$  be the dimension of the domain of the functions to be interpolated; then for each  $\ell = 1, \dots, d$  consider a set of interpolating functions  $\{b_i^{(\ell)}(x)\}$  over  $n_\ell + 1$  nodes  $x_i$  in an interval  $I_\ell$  such that

$$b_i^{(\ell)}(x_k) = \delta_{i,k}$$

and forming the one-dimensional linear interpolant

$$\mathcal{I}_{n_\ell}^\ell f(x) = \sum_{i=0}^{n_\ell} f(x_i) b_i^{(\ell)}(x).$$

To construct a  $d$ -dimensional tensor product interpolation operator of a multivariate function

$$f := f(\xi_1, \dots, \xi_d), \quad f : I^d \rightarrow \mathbb{R}$$

in the box  $I^d = I_1 \times \dots \times I_d$ , we consider the operator

$$\mathcal{I} : \mathcal{C}(I^d) \rightarrow \mathcal{C}(I^d), \quad \mathcal{I} = \mathcal{I}_{n_1}^1 \otimes \dots \otimes \mathcal{I}_{n_d}^d,$$

where  $\mathcal{I}_{n_j}^j$  is a one dimensional linear interpolation operator over a set of nodes  $x_i^{(j)} \in I_\ell$ , with  $i = 0, \dots, n_\ell$ . Then, the tensor product interpolant is of the form (see e.g. [26, p. 30])

$$(\mathcal{I}f)(\xi_1, \dots, \xi_d) = \sum_{i_1=0}^{n_1} \dots \sum_{i_d=0}^{n_d} f(x_{i_1}^{(1)}, \dots, x_{i_d}^{(d)}) b_{i_1}^{(1)}(\xi_1) \dots b_{i_d}^{(d)}(\xi_d). \quad (9)$$

We will now focus on the case  $d = 2$  and the domain

$$B = [0, 2] \times [0, 2\pi]. \quad (10)$$

Starting with the first interval, we let  $\mathcal{X}_n$  be the set of nodes, in  $[0, 2]$ , and use the basis functions

$$b_i^{(1)}(r) = \frac{(-1)^i \delta_i \eta_i}{\sum_{j=0}^{n_1} \frac{(-1)^j \delta_j \eta_j}{r - r_j}},$$

in radial direction, where  $\delta_i$  is as (2) and  $\eta_i$  defined by

$$\eta_i := \begin{cases} \sqrt{1 - (x_i - 1)^2}, & 0, 2 \notin \mathcal{X}_n, \\ \sqrt{\frac{1 + (x_i - 1)^2}{2}}, & 0 \notin \mathcal{X}_n, 2 \in \mathcal{X}_n, \\ \sqrt{\frac{1 - (x_i - 1)^2}{2}}, & 0 \in \mathcal{X}_n, 2 \notin \mathcal{X}_n, \\ 1, & 0, 2 \in \mathcal{X}_n. \end{cases} \quad (11)$$

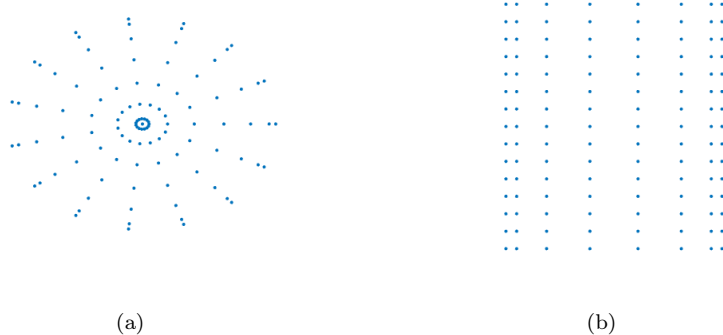


Figure 1: An example of grid with  $n_1 = 7$  and  $n_2 = 15$ , in the disk and in the rectangle  $B$

In the angular direction we take the periodic basis

$$b_i^{(2)}(\phi) = \frac{(-1)^i \text{cst} \left( \frac{\phi - \phi_i}{2} \right)}{\sum_{j=0}^{n_2-1} (-1)^j \text{cst} \left( \frac{\phi - \phi_j}{2} \right)}.$$

on  $[0, 2\pi)$ . This leads on two-dimensional domains to the tensor product

$$\mathcal{I} = R_1 \otimes t_n$$

of Berrut's second interpolant  $R_1$  and the trigonometric interpolant  $t_n$  introduced in [7] as well, and is an operator from the space of continuous functions in  $B$  to  $\mathcal{R}_n \otimes \Sigma_n$ , where  $\mathcal{R}_n$  is the space of rational interpolants with the fixed denominator  $\sum_{j=0}^{n_1} ((-1)^j \delta_j \eta_j) / (x - x_j)$  and  $\Sigma_n$  is the space of rational trigonometric functions of degree  $\lfloor \frac{n_2}{2} \rfloor$  with the same fixed denominator  $\sum_{j=0}^{n_2-1} (-1)^j \text{cst} \left( \frac{\phi - \phi_j}{2} \right)$ .

Note that, since the second basis functions are periodic, this interpolant can be seen as one in polar coordinates in the disk

$$E = \{x \in \mathbb{R}^2 : \|x\|_2 \leq 2\}. \quad (12)$$

To take advantage of the rapid unidimensional convergence and good conditioning of those interpolants, we will consider as nodes the direct product of Chebyshev points of the second kind in  $[0, 2]$ ,

$$r_i = -\cos \left( \frac{i\pi}{n_1} \right) + 1, \quad i = 0, \dots, n_1,$$

and equidistant nodes in  $[0, 2\pi)$ ,

$$\theta_j = j \cdot \frac{2\pi}{n_2}, \quad j = 0 \dots, n_2 - 1.$$

Therefore, the interpolant will be of the form

$$\mathcal{I}[f](r, \theta) = \frac{\sum_{i=0}^{n_1} \prod_{j=0}^{n_2-1} \frac{(-1)^{i+j}}{r-r_i} \text{cst} \left( \frac{\theta - \theta_j}{2} \right) f(r_i, \theta_j)}{\sum_{i=0}^{n_1} \prod_{j=0}^{n_2-1} \frac{(-1)^{i+j}}{r-r_i} \text{cst} \left( \frac{\theta - \theta_j}{2} \right)}. \quad (13)$$

Note that using these bases allows us to consider conformally shifted nodes in the two variables and thus the interpolant

$$\mathcal{I}[f](r, \theta) = \frac{\sum_{i=0}^{n_1} \prod_{j=0}^{n_2-1} \frac{(-1)^{i+j}}{g_1(r)-g_1(r_i)} \text{cst} \left( \frac{g_2(\theta)-g_2(\theta_j)}{2} \right) f(g_1(r_i), g_2(\theta_j))}{\sum_{i=0}^{n_1} \prod_{j=0}^{n_2-1} \frac{(-1)^{i+j}}{g_1(r)-g_1(r_i)} \text{cst} \left( \frac{g_2(\theta)-g_2(\theta_j)}{2} \right)} \quad (14)$$

with the two unidimensional conformal maps

$$g_1 : [0, 2] \rightarrow [0, 2] \quad \text{and} \quad g_2 : [0, 2\pi) \rightarrow [0, 2\pi).$$

This will allow us to use conformal maps to cluster nodes near a given location  $(\bar{r}, \bar{\theta})$ , for example by using the Bayliss-Turkel map [5] as  $g_1$  and the map introduced by the authors in [8] as  $g_2$ .

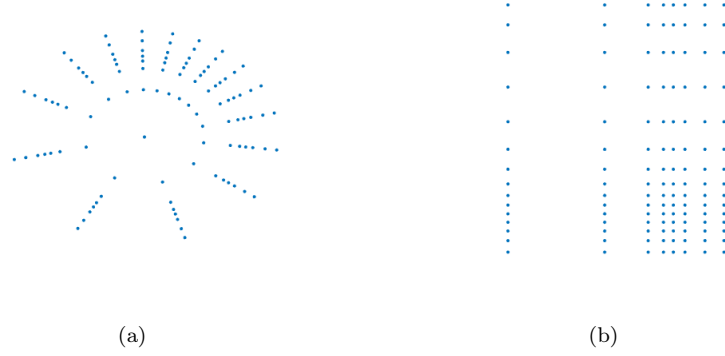


Figure 2: An example of grid with shifted nodes clustered around  $(0.75, \pi/3)$  in the circle and the rectangle  $B$  by using the Bayliss-Turkel map for  $r$  and the map introduced in [8] for  $\theta$  and with  $n_1 = 7$  and  $n_2 = 15$

Then, considering the interpolant  $\mathcal{I}$  over a grid of  $(n_1 + 1)n_2$  nodes in  $[0, 2] \times [0, 2\pi)$ , we can reorder the basis functions from  $(0, 0)$  to  $(n_1, n_2 - 1)$  according to

$$(0, 0) \rightarrow 0, \quad (0, 1) \rightarrow 1, \quad (0, 2) \rightarrow 2, \dots, (n_1, n_2 - 1) \rightarrow n_1(n_2 - 1)$$

and write the interpolant (13) in the linear form

$$\mathcal{I}f(r, \theta) = \sum_{j=0}^{n_1(n_2-1)} B_{i_j}(r, \theta) f(r_{i_j}, \theta_{i_j})$$

with

$$B_{i_j}(r, \theta) = b_{i_j}^{(1)}(r) b_{i_j}^{(2)}(\theta).$$

The Lebesgue constant of  $\mathcal{I}$  is [28, p. 24]

$$\Lambda_{n_1 n_2} = \max_{(r, \theta) \in [0, 2] \times [0, 2\pi)} \sum_{i_j=0}^{n_1(n_2-1)} |B_{i_j}(r, \theta)|,$$

which is equivalent to

$$\begin{aligned}\Lambda_{n_1 n_2} &= \max_{(r, \theta) \in [0, 2] \times [0, 2\pi]} \sum_{i=0}^{n_1} \sum_{j=0}^{n_2-1} |b_i^{(1)}(r)| \cdot |b_j^{(2)}(\theta)| \\ &= \left( \max_{r \in [0, 2]} \sum_{i=0}^{n_1} |b_i^{(1)}(r)| \right) \left( \max_{\theta \in [0, 2\pi]} \sum_{i=0}^{n_2-1} |b_i^{(2)}(\theta)| \right) = \Lambda_{n_1}^{(1)} \Lambda_{n_2}^{(2)},\end{aligned}$$

where  $\Lambda_{n_1}^{(1)}$  is the Lebesgue constant of the interpolant  $R_1$  at the  $n_1 + 1$  nodes  $r_i$  and  $\Lambda_{n_2}^{(2)}$  is that one of  $t_n$  at the  $n_2$  nodes  $\theta_j$  and with the last equality valid since the variables are separate and the maximum is in a rectangle.

With the results from [6] and [9], this proves the following.

**Theorem 7.** *The Lebesgue constant of the interpolant (13) at  $n_1 + 1$  Chebyshev nodes times  $n_2$  equispaced nodes as well as that of the interpolant (14) at conformally shifted nodes obey*

$$\Lambda_{n_1 n_2} = \mathcal{O}(\log n_1 \log n_2).$$

### 3 Interpolation on two-dimensional starlike domains

We shall now consider functions on starlike domains [12, p. 92].

**Definition 1.** *A domain  $\Omega \subset \mathbb{R}^2$  is called starlike with respect to a point  $x \in \Omega$ , if for every point  $y \in \Omega$  the closed segment  $[x, y]$  is contained in  $\Omega$ .*

**Definition 2.** *A domain  $\Omega \subset \mathbb{R}^2$  is called starlike, if it is starlike with respect to at least one of its points.*

In particular, we are going to focus on a specific type of starlike domains that corresponds to a deformation of the unit circle. We shall write  $\Omega$  in polar coordinates where we take  $(0, 0)$  as the center of the domain, i.e., as the domain contained in the curve

$$z(\theta) := \left( \rho(\theta) \cos(\theta), \rho(\theta) \sin(\theta) \right)$$

for a  $2\pi$ -periodic boundary function

$$\rho(\theta) : [0, 2\pi] \rightarrow \mathbb{R}^{>0},$$

i.e.,

$$\Omega := \left\{ (r, \theta) \in \mathbb{R}^2 : r < \rho(\theta) \right\}.$$



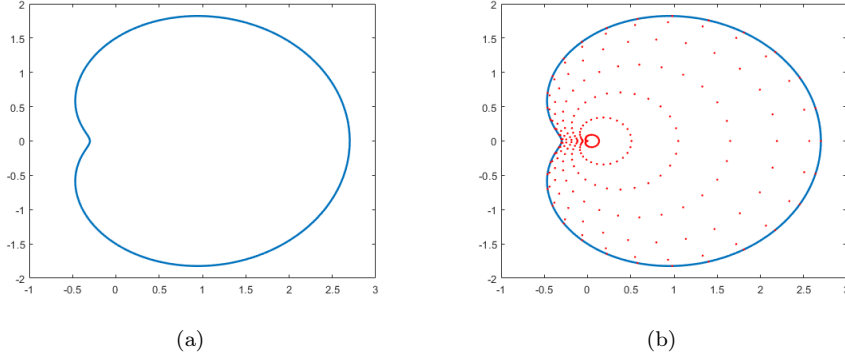


Figure 3: On the left, an example of a starlike domain, namely a limaçon, and on the right an example of the kind of grids used on it

Our goal is to approximate a function  $f$  on  $\bar{\Omega}$  by using the interpolant  $\mathcal{I}$  of the former section. To that aim, we consider the homothetic grid of points in  $\bar{\Omega}$ , which consists in the grid (see the example in Figure 3)

$$G_{i,j} = \left( r_i \rho(\theta_j), \theta_j \right) := \left( \xi_{i,j}, \phi_j \right) \in \bar{\Omega},$$

with the corresponding function values

$$f_{i,j} = f(\xi_{i,j}, \phi_j),$$

and we introduce the change of variable from  $\bar{\Omega}$  to the disk  $E$  (12)

$$S(\xi, \phi) = \left( \frac{2\xi}{\rho(\phi)}, \phi \right) = \left( S_1(\xi, \phi), S_2(\xi, \phi) \right) := (r, \theta). \quad (15)$$

In this way we can interpolate on  $E$  using the data of the function on the grid on  $\bar{\Omega}$  by the function

$$\mathcal{I}[f](S(\xi, \phi)) = \frac{\sum_{i=0}^{n_1} \prod_{j=0}^{n_2-1} \frac{(-1)^{i+j}}{S_1(\xi, \phi) - S_1(\xi_{i,j}, \phi_j)} \text{cst} \left( \frac{S_2(\xi, \phi) - S_2(\xi_{i,j}, \phi_j)}{2} \right) f_{i,j}}{\sum_{i=0}^{n_1} \prod_{j=0}^{n_2-1} \frac{(-1)^{i+j}}{S_1(\xi, \phi) - S_1(\xi_{i,j}, \phi_j)} \text{cst} \left( \frac{S_2(\xi, \phi) - S_2(\xi_{i,j}, \phi_j)}{2} \right)}. \quad (16)$$

This is similar to a technique introduced by De Marchi et al. [17, 16, 10] called the Fake Nodes (or mapped basis) Approach, which consists in considering the interpolant constructed on the mapped interpolation nodes and a set of evaluation points, mapped as well.

The interpolant (16) inherits several nice properties from the interpolant (13).

**Proposition 1.** *Let  $S$  be as in (15). Then the Lebesgue constant  $\bar{\Lambda}_{n_1 n_2}$  of the interpolant (16) at the set of nodes  $G_{i,j}$  satisfies*

$$\bar{\Lambda}_{n_1 n_2} = \mathcal{O}(\log n_1 \log n_2).$$

*Proof.* By definition, the Lebesgue constant of (16) is

$$\begin{aligned}\bar{\Lambda}_{n_1 n_2} &= \max_{(\xi, \phi) \in \bar{\Omega}} \sum_{i_j=0}^{n_1(n_2-1)} |B_{i_j}(S(\xi, \phi))| = \max_{(r, \theta) \in S(\bar{\Omega})} \sum_{i_j=0}^{n_1(n_2-1)} |B_{i_j}(r, \theta)| \\ &= \max_{(r, \theta) \in E} \sum_{i_j=0}^{n_1(n_2-1)} |B_{i_j}(r, \theta)| = \Lambda_{n_1 n_2},\end{aligned}$$

where  $\Lambda_{n_1 n_2}$  is the Lebesgue constant of the interpolant (13). Theorem 7 then yields the result.  $\square$

Note that this is true in particular when the points  $G_{i,j}$  are such that their images under the map  $S$  are conformally shifted nodes in the disk.

Moreover, we may consider the effect of perturbed data  $\tilde{f}(G_{i,j})$  on the interpolant.

**Proposition 2.** *Let  $S$  and the interpolant  $\mathcal{I}[f]$  be as above and consider perturbed data  $\tilde{f}$ . Then,*

$$\max_{(\xi, \phi) \in \bar{\Omega}} |\mathcal{I}[f](\xi, \phi) - \mathcal{I}[\tilde{f}](\xi, \phi)| \leq \Lambda_{n_1 n_2} \max_{(\xi, \phi) \in \bar{\Omega}} |f(\xi, \phi) - \tilde{f}(\xi, \phi)|.$$

*Proof.* This follows directly from Proposition 1 and the classical estimate on the conditioning of an interpolant (see e.g. [28, p. 23]), i.e.,

$$\left\| p_n[f] - p_n[\tilde{f}] \right\| \leq \Lambda_n \left\| f - \tilde{f} \right\|,$$

with  $p_n[h]$  the polynomial of degree at most  $n$  which interpolates the function  $h$  at a fixed set of nodes and  $\Lambda_n$  the norm of the interpolation operator.  $\square$

## 4 Convergence

In order to study its convergence in a starlike domain, we first consider the interpolant in the disk (or the rectangle). For that purpose, we shall make the following assumption.

**Assumption 1.** *Given a function  $f \in \mathcal{C}^\infty(B)$ , where  $B$  is as in (10), such that for any fixed  $r$  the function  $f(r, \cdot)$  is  $2\pi$ -periodic, assume that there is a  $\sigma > 1$  such that, for each fixed  $\bar{\theta} \in [0, 2\pi]$ , there exists an analytic extension of  $f_1(r) := f(r, \bar{\theta})$  to the ellipse  $\mathcal{E}_\sigma \subset \mathbb{C}$  of foci 0 and 2 and with the sum of the lengths of the semiminor and semimajor axes equal to  $\sigma$ , say  $\tilde{f}_1(r)$ , bounded in  $\mathcal{E}_\sigma$  by a certain constant  $M_1 > 0$ , independent of  $\bar{\theta}$ . Furthermore, assume that there is an  $a > 0$  such that, for each fixed  $\bar{r} \in [0, 2]$ , there exists an analytic extension of  $f_2(\theta) := f(\bar{r}, \theta)$  to a strip  $S_a = \{\text{Im}(w) \leq a\} \subset \mathbb{C}$ , say  $\tilde{f}_2(\theta)$ , bounded in  $S_a$  by a certain constant  $M_2 > 0$ , independent of  $\bar{r}$ .*

Let us denote

$$\|f\| := \max_{(r, \theta) \in B} |f(r, \theta)|.$$

Under Assumption 1 we can prove the following bound.

**Theorem 8.** For a function  $\mathcal{C}^\infty(B)$ , let Assumption 1 be satisfied. Then the error of the interpolant (13) can be bounded as

$$\|f - \mathcal{I}[f]\| \leq \left(2\Lambda_{n_1}^{(1)} + \Lambda_{n_1}^{(1)}\Lambda_{n_2}^{(2)} + 1\right) \max \left\{ \frac{4M_1}{\sigma - 1} \sigma^{-n_1}, 2M_2 \operatorname{ctg} \left( \frac{a}{2} \right) e^{-an_2} \right\}. \quad (17)$$

*Proof.* First, let us consider the points  $(\bar{r}, \bar{\theta}) \in B$  such that

$$(\bar{r}, \bar{\theta}) = \arg \max_{(r, \theta) \in B} |f(r, \theta) - \mathcal{I}[f](r, \theta)|.$$

Then, with the notations

$$\mathcal{I}_1[f](r, \theta) := \sum_{i=0}^{n_1} b_i^{(1)}(r) f(r_i, \theta) \quad \text{and} \quad \mathcal{I}_2[f](r, \theta) := \sum_{j=0}^{n_2-1} b_j^{(2)}(\theta) f(r, \theta_j),$$

we can compute

$$\begin{aligned} \|f - \mathcal{I}[f]\| &= \left| f(\bar{r}, \bar{\theta}) - \mathcal{I}[f](\bar{r}, \bar{\theta}) \right| = \left| f(\bar{r}, \bar{\theta}) - \mathcal{I}_1[\mathcal{I}_2[f]](\bar{r}, \bar{\theta}) \right| \\ &= \left| f(\bar{r}, \bar{\theta}) - \mathcal{I}_1[f](\bar{r}, \bar{\theta}) + \mathcal{I}_1[f](\bar{r}, \bar{\theta}) - \mathcal{I}_1[\mathcal{I}_2[f]](\bar{r}, \bar{\theta}) \right| \\ &\leq \left| f(\bar{r}, \bar{\theta}) - \mathcal{I}_1[f](\bar{r}, \bar{\theta}) \right| + \left| \mathcal{I}_1[f](\bar{r}, \bar{\theta}) - \mathcal{I}_1[\mathcal{I}_2[f]](\bar{r}, \bar{\theta}) \right| \\ &= \left| f(\bar{r}, \bar{\theta}) - \mathcal{I}_1[f](\bar{r}, \bar{\theta}) \right| + \left| \mathcal{I}_1[f(\cdot, \bar{\theta}) - \mathcal{I}_2[f](\cdot, \bar{\theta})](\bar{r}) \right|, \end{aligned}$$

where the last line holds in view of the the linearity of  $\mathcal{I}_1$ . Thus,

$$\begin{aligned} \|f - \mathcal{I}[f]\| &\leq \left| f(\bar{r}, \bar{\theta}) - \mathcal{I}_1[f](\bar{r}, \bar{\theta}) \right| + \|\mathcal{I}_1\| \left| f(\bar{r}, \bar{\theta}) - \mathcal{I}_2[f](\bar{r}, \bar{\theta}) \right| \\ &\leq (1 + \Lambda_{n_1}^{(1)}) \frac{4M_1}{\sigma - 1} \sigma^{-n_1} + \Lambda_{n_1}^{(1)} (1 + \Lambda_{n_2}^{(2)}) 2M_2 \operatorname{ctg} \left( \frac{a}{2} \right) e^{-an_2}, \end{aligned}$$

where we have used the classic estimate for interpolation [28, p. 24]

$$\|h - p_n[h]\| \leq (1 + \Lambda_n) \|h - p^*\|,$$

where  $p^*$  denotes the best approximation of  $h$  in  $\mathbb{P}_n$  and the fact that, since  $\mathcal{I}_1$  (respectively  $\mathcal{I}_2$ ) corresponds to the interpolation at Chebyshev nodes of the second kind (resp. trigonometric interpolation at equidistant nodes) we have from Theorem 2 that, for a function  $h : \mathbb{R} \rightarrow \mathbb{R}$  analytic in the ellipse  $\mathcal{E}_\sigma$ ,

$$\|h - p^*\| \leq \|h - \mathcal{I}_1[h]\| \leq \frac{4M_1}{\sigma - 1} \sigma^{-n_1},$$

and similarly for  $\mathcal{I}_2$  with Theorem 5.

Therefore, we have (17). □

Similarly we can prove a convergence theorem with weaker conditions by using Theorems 1 and 4. To that end, let us introduce the following assumption.

**Assumption 2.** Given a function  $f$  in  $B$  such that for any fixed  $r$  the function  $f(r, \cdot)$  is  $2\pi$ -periodic, assume that there exists an integer  $\nu \geq 1$  such that, for each fixed  $\theta \in [0, 2\pi]$ ,  $f_1(r) := f(r, \theta)$  and its derivatives are absolutely continuous up to  $f_1^{(\nu-1)}$  and the  $\nu^{\text{th}}$ -derivative is of bounded variation with its total variation smaller or equal than  $V_1$ . Furthermore, assume that there exists a  $\mu$  such that the function  $f_2(\theta) := f(\bar{r}, \theta)$  has for each fixed  $\bar{r} \in [0, 2]$  at most simple jump discontinuities in the  $\mu^{\text{th}}$  derivative and  $f_2^{(\mu)}$  is of bounded variation with a total variation smaller than or equal to  $V_2$ .

We then have the following bound, by proceeding as in the proof of Theorem 8.

**Theorem 9.** For a function  $f$  such that Assumption 2 is satisfied, we can bound the error of the interpolant (13) as

$$\|f - \mathcal{I}[f]\| \leq \left(2\Lambda_{n_1}^{(1)} + \Lambda_{n_1}^{(1)}\Lambda_{n_2}^{(2)} + 1\right) \max \left\{ \frac{4V_1}{\pi\nu(n-\nu)^\nu}, \frac{V_2}{\pi n^\mu} \left(\frac{1}{n} + \frac{2}{\mu}\right) \right\}. \quad (18)$$

We shall obtain similar bounds for the interpolant at conformally shifted nodes under the following assumption.

**Assumption 3.** Here we suppose we are given a function  $f \in C^\infty(B)$ , where  $B$  is (10), and such that for each fixed  $r$  the function  $f(r, \cdot)$  is  $2\pi$ -periodic and given two conformal maps  $g_1$  and  $g_2$  such that  $g_1 : \mathcal{D}_1 \rightarrow \mathcal{D}_2$ , with  $\mathcal{D}_1$  and  $\mathcal{D}_2$  two domains in  $\mathbb{C}$  such that the interval  $[0, 2]$  is mapped into itself and  $g_2$  is a periodic function such that  $w(\phi, \theta) = \text{cst} \left( \frac{g(\phi) - g(\theta)}{2} \right) / \text{cst} \left( \frac{\phi - \theta}{2} \right)$  is bounded and analytic in  $S_a \times S_a$ , with  $S_a = \{|\text{Im}(w)| \leq a\} \subset \mathbb{C}$  for an  $a > 0$ , and such that the interval  $[0, 2\pi]$  is mapped into itself. Further, assume that there is a  $\sigma > 1$  such that there exists an analytic extension  $\tilde{f}_1(r)$  of the composition  $(f_1 \circ g_1)(r) := f(g_1(r), \theta)$  to the ellipse  $\mathcal{E}_\sigma \subset \mathbb{C}$  of foci 0 and 2 and with the sum of the lengths of the semiminor and semimajor axes equal to  $\sigma$ , bounded in  $\mathcal{E}_\sigma$  by a certain constant  $M_1 > 0$  for each fixed  $\theta \in [0, 2\pi]$  and independent of  $\theta$ . Assume further that there exists an analytic extension  $\tilde{f}_2(\theta)$  of the composition  $(f_2 \circ g_2)(\theta) := f(\bar{r}, g_2(\theta))$  to a strip  $S_a$ , bounded in  $S_a$  by a certain constant  $M_2 > 0$  for each fixed  $\bar{r} \in [0, 2]$  and independent of  $\bar{r}$ .

Then, following the proof of Theorem 8 but estimating with the best approximation in the spaces  $\mathcal{R}_n$  and  $\Sigma_n$  introduced in section 2, instead of the best approximation in the space of polynomials, and using Theorems 3 and 6, we obtain the following bound on the interpolant at conformally shifted nodes.

**Theorem 10.** For a function  $f \in C^\infty(B)$ , let Assumption 3 be satisfied. Then, we can bound the error of the interpolant (14) as

$$\|f - \mathcal{I}[f]\| \leq \left(2\Lambda_{n_1}^{(1)} + \Lambda_{n_1}^{(1)}\Lambda_{n_2}^{(2)} + 1\right) \max \{C_1\sigma^{-n_1}, C_2e^{-an_2}\}, \quad (19)$$

for two constants  $C_1, C_2$ , where  $C_1$  depends on  $\sigma$  and  $g_1$ ,  $C_2$  on  $a$  and  $g_2$ , and both on the function  $f$ .

Finally, note that the interpolant in the starlike domain inherits the error from the interpolant on the disk.

**Theorem 11.** *Let  $S$  be as in (15),  $\mathcal{I}$  as in (13) (or (14)), and  $\mathcal{I}^S$  as in (16). Then for a function  $f : \Omega \rightarrow \mathbb{R}$  we have*

$$\|f - \mathcal{I}^S[f]\|_{\Omega} = \|h - \mathcal{I}[h]\|_E, \quad (20)$$

where  $h = f \circ S^{-1}$ .

*Proof.* By definition we have  $\mathcal{I}^S = \mathcal{I} \circ S$ ; then, if we consider as  $h$  the function such that  $h \circ S = f$ , we have

$$\|\mathcal{I}^S[f] - f\|_{\Omega} = \|\mathcal{I} \circ S - h \circ S\|_{\Omega} = \|\mathcal{I}[h] - h\|_{S(\Omega)},$$

and  $S(\Omega) = E$ . □

Consequently, since the interpolant converges as that of the function  $h = f \circ S^{-1}$ , where

$$S^{-1}(r, \theta) := \left( \frac{r\rho(\theta)}{2}, \theta \right),$$

the convergence depends on  $f$  and  $S$ ; a smoother function  $\rho$  will lead to a better interpolant (16) of the function  $f$  in  $\bar{\Omega}$ .

We have also interpolated in non-smooth domains but the results were not satisfactory, as the function  $h$  itself is non-smooth along the boundary, i.e., for  $r = 2$ .

A way of dealing with such non-smooth functions  $\rho$ , as for example the polar representation of the square

$$\rho(\theta) = \min \left\{ \frac{1}{|\cos(\theta)|}, \frac{1}{|\sin(\theta)|} \right\}, \quad (21)$$

is to replace it with a close enough smoother approximant  $\tilde{\rho}$  and interpolate in the approximate domain  $\tilde{\Omega} = \tilde{S}(E)$  instead of  $\bar{\Omega} = S(E)$ , where  $\tilde{S}$  is the function  $S$  with  $\tilde{\rho}$  in place of  $\rho$ . Some tests in this direction are reported in the next section.

## 5 Numerical tests

In this section we test the interpolant

$$\mathcal{I}[f](S(\xi, \phi)) = \frac{\sum_{i=0}^{n_1} \prod_{j=0}^{n_2-1} \frac{(-1)^{i+j}}{S_1(\xi, \phi) - S_1(\xi_{i,j}, \phi_j)} \text{cst} \left( \frac{S_2(\xi, \phi) - S_2(\xi_{i,j}, \phi_j)}{2} \right) f_{i,j}}{\sum_{i=0}^{n_1} \prod_{j=0}^{n_2-1} \frac{(-1)^{i+j}}{S_1(\xi, \phi) - S_1(\xi_{i,j}, \phi_j)} \text{cst} \left( \frac{S_2(\xi, \phi) - S_2(\xi_{i,j}, \phi_j)}{2} \right)},$$

on domains inside the curve

$$z(\theta) := \left( \rho(\theta) \cos(\theta), \rho(\theta) \sin(\theta) \right),$$

for a  $2\pi$ -periodic boundary parametrization

$$\rho(\theta) : [0, 2\pi] \rightarrow \mathbb{R}^{>0}.$$

We first consider the following domains (see Figure 4):

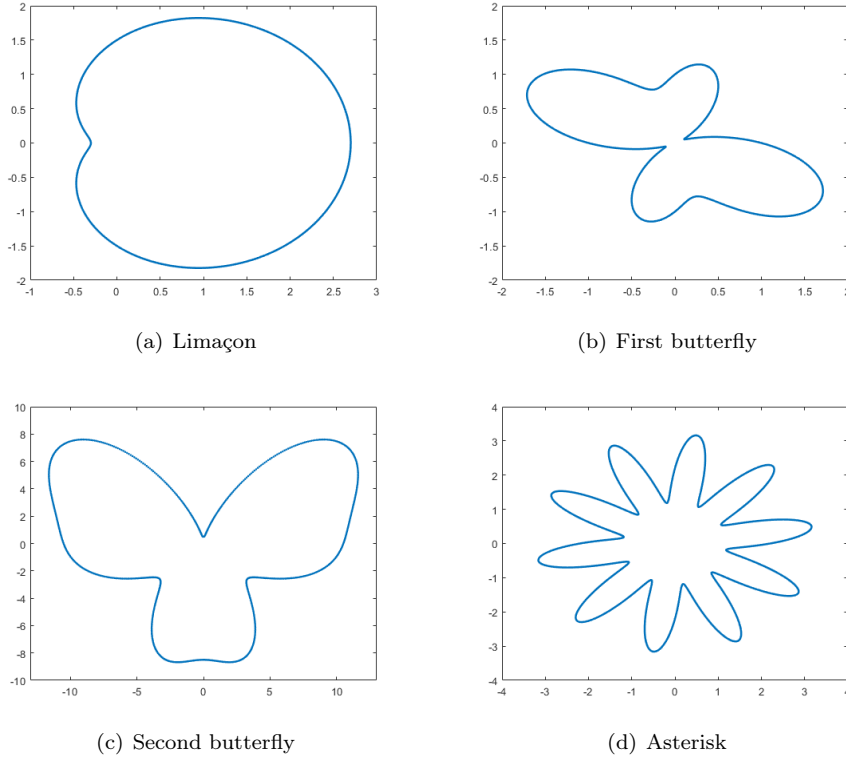


Figure 4: Test domains

- The limaçon

$$\rho_1(\theta) = 1.5 + 1.2 \cos(\theta);$$

- A first butterfly-shaped domain

$$\rho_2(\theta) = 1 - \cos(\theta) \sin(3\theta);$$

- A second butterfly-shaped domain

$$\rho_3(\theta) = 7.5 - \sin(\theta) + 4 \sin(3\theta) - \sin(7\theta) + 3 \cos(2\theta);$$

- The asterisk

$$\rho_4(\theta) = \sin(10\theta) + 2.2.$$

To estimate the error, we consider a grid of  $170 \times 170$  uniformly spaced points in a rectangle around the domain (see Table 1 for the rectangles) and we filter them by considering only the points inside the domain. Then, we compute the maximum of the absolute value of the difference between the interpolant and the function in these points.

Notice that all these domains are constructed via a smooth function  $\rho$ ; thus the expected convergence behaviour will not be influenced by infinitely smooth changes of variable such as conformal point shifts.

	Rectangle
$\rho_1$	$[-1, 3] \times [-2, 2]$
$\rho_2$	$[-2, 2] \times [-2, 2]$
$\rho_3$	$[-13, 13] \times [-10, 10]$
$\rho_4$	$[-4, 4] \times [-4, 4]$
$\rho_5$	$[-2, 2] \times [-2, 2]$

Table 1: Rectangles for the various domains

$(n_1, n_2)$	$\rho_1$	$\rho_2$	$\rho_3$	$\rho_4$
(10,30)	1.6762e-02	1.3439e-01	1.4178e+01	2.8832e+01
(20,60)	1.6080e-07	3.3468e-04	2.1093e+00	3.0920e+00
(40,120)	8.5265e-14	1.3499e-10	9.0279e-02	1.5704e-02
(80,240)	1.2790e-13	7.1054e-14	2.0515e-05	4.6051e-07
(160,480)	1.4921e-13	1.0303e-13	9.9476e-14	5.6843e-13

Table 2: Error with the function  $f_1$

Firstly, let us consider the smooth analytic function

$$f_1(x, y) = 3e^{-x^2+y+1} + 3,$$

for which we expect (approximate) exponential convergence. As we observe in Table 2, each error is approximately the square of that on the previous row when  $(n_1, n_2)$  is doubled; this indeed reflects an exponential decay of the error.

As mentioned in Section 3, a big advantage of linear barycentric rational interpolation is its ability to accommodate steep gradients (fronts) by simply replacing the nodes in the "classical" interpolant with shifted ones which accumulate in the vicinity of the fronts. To demonstrate this, we use the interpolant  $\mathcal{I}[f]$  in (16) and we consider secondly a function with a front in a precise location, i.e.,

$$f_2(x, y) = 40 \frac{\operatorname{erf}\left(\sqrt{\epsilon/2}(x+0.6)\right)}{\operatorname{erf}\left(\sqrt{\epsilon/2}\right)} e^{-30(x+0.6)^2} e^{-60(y-0.6)^2},$$

where  $\epsilon = 100$  and  $\operatorname{erf}$  is the error function;  $f_2$  has a front in  $(-0.6, 0.6)$  ( $(0.6\sqrt{2}, \frac{7\pi}{4})$  in polar coordinates). We use the conformal maps

$$g_1 = \beta + \frac{1}{\alpha} \tan(\lambda(x - \mu)), \quad \text{and} \quad g_2(\theta) = -i \log \left( \frac{e^{i\phi} + \eta e^{i\theta}}{1 + e^{i\phi} \eta e^{-i\theta}} \right)$$

with  $\beta$  and  $\phi$  such that the nodes cluster around the location of the front and for the density  $\alpha = 2.8$  for  $g_1$  and  $\eta = 0.65$  for  $g_2$ ;  $g_1$  and  $g_2$  are respectively the Bayliss-Turkel map [5] and the map introduced by the authors in [8]. The results, displayed in Tables 3 and 4, indeed show that, as in the unidimensional case, we achieve a much faster convergence by using conformal maps to cluster nodes in the vicinity of the location of a front instead of the Chebyshev and equispaced points.

Furthermore, we consider a domain which corresponds to a non-smooth function  $\rho$ , the square  $[-1, 1]^2$ , parametrized by the function (21) which we denote by  $\rho_5$ .

$(n_1, n_2)$	$\rho_1$	$\rho_1$ conf	$\rho_2$	$\rho_2$ conf
(10,30)	2.2524e+01	4.9054e+00	1.7898e+01	1.8408e+00
(20,60)	7.7530e+00	1.7487e-02	4.6606e+00	3.7443e-02
(40,120)	1.0473e-01	6.2046e-07	6.1903e-02	1.0631e-05
(80,240)	2.2811e-07	1.8474e-13	1.5352e-06	5.8037e-13

Table 3: Error with the function  $f_2$

$(n_1, n_2)$	$\rho_3$	$\rho_3$ conf	$\rho_4$	$\rho_4$ conf
(10,30)	1.8077e+01	1.3739e+01	2.2392e+01	1.3262e+01
(20,60)	7.6290e+00	2.7313e+00	2.1117e+01	5.3838e+00
(40,120)	1.3786e+00	2.6799e-02	1.1580e+01	7.5581e-01
(80,240)	1.9880e-02	1.3075e-06	9.3368e-01	7.3685e-03
(160,480)	2.3293e-08	1.0303e-13	1.5659e-03	1.3545e-08

Table 4: Error with the function  $f_2$

In this case, approximating functions with the mapped interpolant often leads to catastrophic results, see the columns  $\rho_5$  in Table 5. To avoid this, we slightly modify the domain by approximating  $\rho_5$  with a smooth interpolant  $\tilde{\rho}_5$  and we use the interpolant mapped via the function

$$\tilde{S}(\xi, \phi) = \left( \frac{2\xi}{\tilde{\rho}(\phi)}, \phi \right) = \left( \tilde{S}_1(\xi, \phi), \tilde{S}_2(\xi, \phi) \right) := (r, \theta).$$

For Table 5 we approximate  $\rho_5$  via the approximant produced by the AAA algorithm [27]: the corresponding  $\tilde{\rho}_5$  clearly gives a better interpolant than  $\rho_5$ . Unfortunately, because of its "almost corner", the AAA approximant may lead, in practice, to an interpolant with a slower than exponential convergence in the neighbourhood of the corners; furthermore, the interpolation is merely performed in an approximation of the original domain  $[-1, 1]^2$ .

In one last test, we consider a sketch of Switzerland, in which we simplify the boundary in order to have a starlike domain with respect to the origin (see Figure 5). To that end, we extracted some points which we use as nodes to interpolate the unknown function  $\rho_6$  representing the boundary of the "Swiss-like domain".

To approximate this curve, we use Berrut's first interpolant  $R_0$  (see e.g. [7, 25]), which produces an approximation, let us denote it by  $\tilde{\rho}_6$ , of the unknown function  $\rho_6$  (see Figure 6). In this case, the rectangle in which we compute the

$(n_1, n_2)$	$f_1$		$f_2$		
	$\rho_5$	$\tilde{\rho}_5$	$\rho_5$	$\tilde{\rho}_5$	$\tilde{\rho}_5$ conf
(10,30)	2.9917e+00	4.4789e-01	9.3838e+03	1.2996e+01	1.8835e+00
(20,60)	3.1510e+00	2.6646e-01	1.5954e+09	7.4563e+00	1.3315e+00
(40,120)	Inf	7.7975e-02	Inf	1.9865e+00	1.0297e-01
(80,240)	Inf	3.7900e-02	Inf	4.9346e-01	4.0428e-02
(160,480)	Inf	4.8907e-03	Inf	2.1970e-01	8.1943e-03

Table 5: Error with the approximate  $\rho_5$  for the square



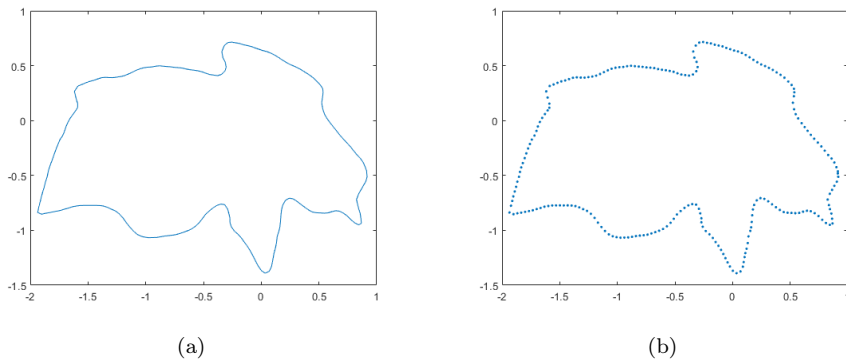


Figure 5: Swiss-like domain: (a) The sketch; (b) The extracted nodes

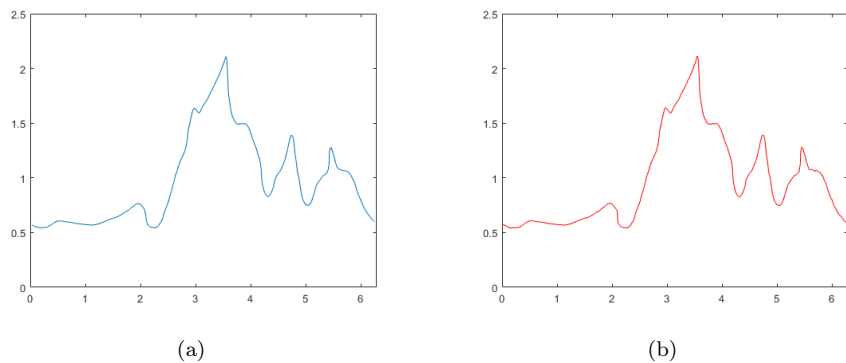


Figure 6: (a)  $\rho_6$ ; (b) The approximation  $\tilde{\rho}_6$

error of the interpolant is  $[-2.5, 1.5] \times [-2, 1.5]$ .

In Table 6 we display the errors produced with the functions  $f_1$  and  $f_2$ ; the exponential convergence does not yet show up without conformal shift, but it does with such a shift.

## 6 Conclusion

The present work has introduced a simple generalisation of linear barycentric rational interpolants to two-dimensional domains. The idea is to parameterize a (starlike) domain with polar coordinates and to use linear barycentric interpolation in radial direction and its trigonometric version in circular (homothetic) direction. (In reality, the interpolation happens in a disk, to which the original problem is transplanted.) Up to a logarithmic factor (which arises from the proof, but may not appear in practice), the resulting tensor-product-like interpolant converges exponentially when the function is analytic, and as  $\mathcal{O}(h^\nu)$  when  $f^{(\nu)}$  has bounded variation. Impressive numerical examples amply confirm these theoretical convergence results.

$(n_1, n_2)$	$f_1$	$f_2$	
	$\tilde{\rho}_6$	$\tilde{\rho}_6$	$\tilde{\rho}_6$ conf
(40,120)	4.3451e-01	9.6853e+00	5.3945e+00
(80,240)	3.2449e-01	9.2768e+00	6.3695e-01
(160,480)	1.5968e-01	6.2080e+00	3.0078e-01
(320,960)	4.1611e-02	1.3068e+00	2.6339e-02
(640,1920)	1.9271e-02	4.1124e-01	8.5433e-05
(1280,3840)	1.7645e-03	5.4788e-02	1.0787e-09

Table 6: Error with the approximate  $\rho_6$

We do not want to conceal some limitations of the method. The most important seems to be the fact that the rapid convergence requires that the boundary parametrization is as smooth as the interpolated function  $f$ , as the interpolant involves the trigonometric interpolation of  $f$  along the boundary. Another one is the fact that the boundary curve cannot be arbitrary: for instance, its interior must contain a point, to be chosen as the center of the domain, from which the representation of the curve does not have too large a derivative.

Finally, we note that one nice feature of this interpolant is the simplicity of the formulae for its partial derivatives along the lines making up its grid: in radial direction they are given by Schneider and Werner’s formula [30], for the circular direction one finds them in [3] (up to inner derivatives of the variable transformation in the chain rule).

## Acknowledgements

This research has been accomplished within the Rete Italiana di Approssimazione (RITA), the thematic group on Approximation Theory and Applications of the Italian Mathematical Union, and with the support of GNCS-IN $\delta$ AM.

## References

- [1] J. Abouir and A. Cuyt. “Error formulas for multivariate rational interpolation and Padé approximation”. In: *J. Comput. Appl. Math.* 31.2 (1990), pp. 233–241.
- [2] A. P. Austin et al. “Multivariate Rational Approximation”. Preprint, arXiv:1912.02272.
- [3] R. Baltensperger. “Some results on linear rational trigonometric interpolation”. In: *Comput. Math. Appl.* 43 (2002), pp. 737–746.
- [4] R. Baltensperger, J.-P. Berrut, and B. Noël. “Exponential convergence of a linear rational interpolant between transformed Chebyshev points”. In: *Math. Comp.* 68.227 (1999), pp. 1109–1120.
- [5] A. Bayliss and E. Turkel. “Mappings and accuracy for Chebyshev pseudospectral approximations”. In: *J. Comput. Phys.* 101.2 (1992), pp. 349–359.

- [6] J.-P. Berrut. “Conditioning of a linear barycentric rational interpolant”. to appear in *Festschrift in honor of Thanos Antoulas’ 70<sup>th</sup> birthday (Springer)*.
- [7] J.-P. Berrut. “Rational functions for guaranteed and experimentally well-conditioned global interpolation”. In: *Comput. Math. Appl.* 15.1 (1988), pp. 1–16.
- [8] J.-P. Berrut and G. Elefante. “A periodic map for linear barycentric rational trigonometric interpolation”. In: *Appl. Math. Comput.* 371 (2020), pp. 124924, 8.
- [9] J.-P. Berrut and G. Elefante. “Bounding the Lebesgue constant for a Barycentric Rational Trigonometric interpolant at periodic well-spaced nodes”. submitted.
- [10] J.-P. Berrut et al. “Treating the Gibbs phenomenon in barycentric rational interpolation and approximation via the S-Gibbs algorithm”. In: *Appl. Math. Lett.* 103 (2020), pp. 106196, 7.
- [11] L. Bos, S. De Marchi, and M. Vianello. “Polynomial approximation on Lissajous curves in the  $d$ -cube”. In: *Appl. Numer. Math.* 116 (2017), pp. 47–56.
- [12] V.I. Burenkov. *Sobolev Spaces on Domains*. Rechtswissenschaftliche Veröffentlichungen. Vieweg+Teubner Verlag, 1998.
- [13] M. Caliarì, S. De Marchi, and M. Vianello. “Bivariate polynomial interpolation on the square at new nodal sets”. In: *Appl. Math. Comput.* 165.2 (2005), pp. 261–274.
- [14] A. Cuyt and B. M. Verdonk. “Multivariate rational interpolation”. In: *Computing* 34.1 (1985), pp. 41–61.
- [15] S. De Marchi, W. Erb, and F. Marchetti. “Spectral filtering for the reduction of the Gibbs phenomenon for polynomial approximation methods on Lissajous curves with applications in MPI”. In: *Dolomites Res. Notes Approx.* 10.Special Issue (2017), pp. 128–137.
- [16] S. De Marchi et al. “Multivariate approximation at fake nodes”. In: *Appl. Math. Comput.* 391 (2021), p. 125628.
- [17] S. De Marchi et al. “Polynomial interpolation via mapped bases without resampling”. In: *J. Comput. Appl. Math.* 364 (2020), pp. 112347, 12.
- [18] R. A. DeVore and X. M. Yu. “Multivariate rational approximation”. In: *Trans. Amer. Math. Soc.* 293.1 (1986), pp. 161–169.
- [19] W. Erb. “Bivariate Lagrange interpolation at the node points of Lissajous curves—the degenerate case”. In: *Appl. Math. Comput.* 289 (2016), pp. 409–425.
- [20] W. Erb et al. “A survey on bivariate Lagrange interpolation on Lissajous nodes”. In: *Dolomites Res. Notes Approx.* 8.Special Issue (2015), pp. 23–36.
- [21] W. Erb et al. “Bivariate Lagrange interpolation at the node points of non-degenerate Lissajous curves”. In: *Numer. Math.* 133.4 (2016), pp. 685–705.

- [22] M. S. Floater. “Polynomial interpolation on interlacing rectangular grids”. In: *J. Approx. Theory* 222 (2017), pp. 64–73.
- [23] D. Gaier. “Ableitungsfreie Abschätzungen bei trigonometrischer Interpolation und Konjugierten-Bestimmung”. In: *Computing (Arch. Elektron. Rechnen)* 12.2 (1974), pp. 145–148.
- [24] P. Henrici. *Essentials of Numerical Analysis with Pocket Calculator Demonstrations*. Wiley, New York, 1982, pp. vi+409. ISBN: 0-471-05904-8.
- [25] K. Hormann. “Barycentric interpolation”. In: *Approximation theory XIV: San Antonio 2013*. Vol. 83. Springer Proc. Math. Stat. Springer, Cham, 2014, pp. 197–218.
- [26] B. N. Khoromskij. *Tensor Numerical Methods in Scientific Computing*. Berlin, Boston: De Gruyter, 2018.
- [27] Y. Nakatsukasa, O. Sète, and L. N. Trefethen. “The AAA algorithm for rational approximation”. In: *SIAM J. Sci. Comput.* 40.3 (2018), A1494–A1522.
- [28] M.J.D. Powell. *Approximation Theory and Methods*. Cambridge University Press, 1981.
- [29] T.J. Rivlin. *The Chebyshev Polynomials*. A Wiley-Interscience publication. Wiley, New-York, 1974.
- [30] C. Schneider and W. Werner. “Some new aspects of rational interpolation”. In: *Math. Comp.* 47.175 (1986), pp. 285–299.
- [31] L.L. Schumaker. *Spline Functions: Computational Methods*. Society for Industrial and Applied Mathematics, Philadelphia, 2015.
- [32] P. Seshadri et al. “Sparse Robust Rational Interpolation for Parameter-dependent Aerospace Models”. In: *54th AIAA/ASME/ASCE/AHS/ASC Structures, Structural Dynamics, and Materials Conference*. American Institute of Aeronautics and Astronautics, Reston, 2013.
- [33] L. N. Trefethen. *Approximation Theory and Approximation Practice*. Society for Industrial and Applied Mathematics, Philadelphia, 2013.
- [34] G. B. Wright et al. “Extension of Chebfun to periodic functions”. In: *SIAM J. Sci. Comput.* 37.5 (2015), pp. C554–C573.